Arab J Sci Eng (2018) 43:281–293
https://doi.org/10.1007/s13369-017-2679-8

RESEARCH ARTICLE - EARTH SCIENCES

Impact of Seawater Intrusion on the Geochemistry of Groundwater of Gwadar District, Balochistan and Its Appraisal for Drinking Water Quality

Shahid Naseem[1] · Erum Bashir[1] · Pazeer Ahmed[2] · Tahir Rafique[3] · Salma Hamza[4] · Maria Kaleem[1]

Received: 22 November 2016 / Accepted: 11 June 2017 / Published online: 7 July 2017

Abstract Thirty-one groundwater samples were collected from Jiwani, Ganz, Pishukan, Gwadar and Sur Bander, coastal towns of Gwadar District, Balochistan Province, Pakistan. The overall average trend of cationic and anionic distributions is found in the order of $Na^+ > Ca^{2+} > Mg^{2+} > K^+$ and $Cl^- > SO_4^{2-} > HCO_3^- > NO_3^- > CO_3^{2-} > F^-$, respectively. Average ionic composition on Stiff diagram shows $(Na^+ + K^+)$–Cl^- as one of the principal ionic pair, while ionic balance among Mg^{2+}–SO_4^{2-} and Ca^{2+}–$(HCO_3^- + CO_3^{2-})$ have shown an imbalance. On Piper diagram, majority of the groundwater samples in the study area are of NaCl type. The Na^+ versus Cl^-, $Na^+/Na^+ + Cl^-$ versus $Cl^-/\sum$ anions, and Cl versus Cl/HCO_3 ratios signify influence of seawater intrusion in the coastal strip of Gwadar District. The impact of seawater encroachment in the coastal regions has also been proved by hydrochemical facies evolution diagram and Piper plots. Principal component analysis reveals three major factors, whereas high positive loading of Na^+, Ca^{2+}, Mg^{2+}, Cl^-, SO_4^{2-} and TDS reveal association with seawater. Potassium, nitrate and bicarbonate are in other domain; their relation with pH being rather negative. Moreover, fluoride and carbonate should be confined to separate realms, specifying of good relation among the two ions. Concentrations of nitrate and fluoride are found to be higher than the WHO permissible limit and may therefore pose a health threat to the local population.

Keywords Geochemistry · Seawater intrusion · Drinking water quality · Gwadar · Balochistan

✉ Shahid Naseem
sngeo@outlook.com

Erum Bashir
ebahmed@yahoo.com

Pazeer Ahmed
Pazeerahmed@gmail.com

Tahir Rafique
tahirrafique92@yahoo.com

Salma Hamza
dr.salma@bimcs.edu.pk

Maria Kaleem
maaria_kaleem@yahoo.com

1 Department of Geology, University of Karachi, Karachi 75270, Pakistan

2 Groundwater Development, Irrigation Department, Government of Balochistan, Quetta, Pakistan

3 Applied Chemistry Research Centre, PCSIR Laboratories Complex, Off University Road, Karachi 75280, Pakistan

4 Department of Earth and Environmental Sciences, Bahria University Karachi Campus, 13 National Stadium Rd, Karachi 75260, Pakistan

1 Introduction

Gwadar District includes major cities like Jiwani, Pishukan, Gwadar and Sur Bander along the coastal belt of Makran in Balochistan Province of Pakistan. The area not only suffers from acute water scarcity, essential for the substantial development of any region but availability of fresh water too is problematic due to its arid climate. Water quality of this particular area has also been influenced by seawater intrusion. Worldwide, coastal areas normally suffer due to interaction between groundwater and seawater. In this zone, fresh groundwater flows above seawater, with a water transition zone in between them [1,2], and the overuse of groundwater in the coastal area, due to ever increasing population density, therefore results in seawater intrusion into the coastal aquifers.

The ionic composition of groundwater has mainly been controlled by rock weathering and other climatic factors [3,4]; anthropogenic activities are also a substantial source of contamination [5]. It has been observed that the total dissolved inorganic carbon of seawater in coastal Makran region indicates minimum influence of domestic and industrial pollution [6]. In the absence of any substantial contribution from anthropogenic sources, the groundwater chemistry therefore has mainly been influenced by the geogenic sources.

Aquifers in these studied areas are mostly confined within Pliocene–Pleistocene formations and their related soils have pebbles of altered ultramafic rocks, which may possibly be derived from the Wakai Group of Cretaceous age, exposed in the north of the study area [7]. The rocks of this group consisting of shale occur as thin slivers or crushed material derived from ophiolitic mélanges. The ophiolitic bodies may have formed during accretion of the oceanic floor of the Gulf of Oman and its subsequent northward subduction beneath the southern margin of the Eurasian Plate [8]. Wakai Group represents low-K, alkaline to sub-alkaline tholeiites, formed in a subduction setting in which lavas were generated in an island arc or active continental margin environment [9]. Magnesium-bearing groundwater in the area may be probably linked to pebbles of Wakai Group, whereas, Kassi et al. [10] have also mentioned the occurrence of igneous pebbles in the Ispikan Group of Late Cretaceous-Paleocene age.

The high Mg content in the soil and groundwater of the study area is supported by the presence of *Nannorrhops ritchiana* (Mazari Palm) and Pishukan town here is named after the abundance of this plant in its vicinity. *N. ritchiana* is a Mg-flora widely grown in the Khuzdar District of Balochistan Province, where mafic and ultramafic rocks of Bela Ophiolite are exposed [11].

The objective of this study is to examine geochemical characteristics of groundwater in the Gwadar district and its appraisal with reference to WHO Drinking Water Standards. Abundance and distribution of groundwater ions have been discussed in relation to water-rock interaction. Moreover, with reference to long-term planning in the region impact of seawater intrusion has also been evaluated for designing a proper mitigation programme, which may facilitate water supply agencies and erecters of reverse osmosis (RO) plants.

2 Hydrogeology

Gwadar District includes the largest city and district headquarters of coastal Makran belt and is also a port with strategic location, near the mouth of the Persian Gulf and close to Strait of Hormuz, the major oil shipping route. It is an emerging center attracting international community especially after the construction of Gwadar-Kashgar Highway (N-35) to China and other Central Asian countries (Pakistan–China Economic Corridor). The area suffers from acute shortage of fresh water due to arid climate and absence of any large stream system. Laura, Pasao, Faleri, Akara, Gatti, Shadad and Sur Kaur are some of the important ephemeral and intermittent streams of the area (Fig. 1), which originate from the northern hilly terrain and finally discharge to the Arabian Sea into the south. Akara Kaur is the largest stream (~65 km) of the area and bulk water supply has mainly been obtained from a small dam (Arka Kaur), located 25 km north of Gwadar city. The supplied water has been found to be contaminated with high amount of SO_4^{2-} ions, hence is not potable [12].

In the coastal strip of Makran region, sedimentary rocks of Miocene to Pleistocene age exposed, include Talar, Chatti, Ormara and Jiwani formations. Talar is the oldest formation (Late Miocene-Early Pliocene) of the study area, mostly exposed in the northern hilly areas, which mainly consist of fine sand/silt stone, shale, mudstone and some clayey limestone [13]. Thick sequence (1–1.2 km) of overlying Chatti formation of Pliocene age widely exposed from Talar area in the east to Jiwani Town in the west, comprising mudstone, siltstone and marl with fragments of mollusk shells [14]. Ormara formation is mainly consists of soft, poorly consolidated sandy clay with minor amount of conglomeratic bed occur in the upper part [15]. The youngest Jiwani Formation of Late Pleistocene, predominantly composed of shelly and reefal limestone, sandstone and conglomerate [7]. It is mainly exposed around Jiwani town and has been intensely folded and faulted [16].

Groundwater in the study area is mainly confined within silt and sand beds of Pliocene–Pleistocene age. However, some groundwater is also found in the recent consolidated and unconsolidated alluvial deposits (Fig. 1). In majority of the cases, aquifers are of the confined type, separated by shale/mud beds of overlying formations [17]. During rainfalls in hilly areas, water flows from catchment boundaries to valleys. Aquifers in the western part of the study area (JN, DL, PW) are confined in the Jiwani Formation. However in Ganz and Dedillo areas, they are found in Ormara Formation. In the eastern extremity (Sur Bander), aquifers are reported in Chatti Formation (Fig. 1), while rest of the water bodies either within Recent or Sub-recent deposits. The depth of water table varies from place to place but generally within the range of 5–50 m [18].

3 Materials and Methods

3.1 Sampling

The study was carried out in the coastal belt of Gwadar and adjoining areas (Fig. 1) and thirty one groundwater samples were collected from the Jiwani, Ganz, Pishukan, Gwadar and

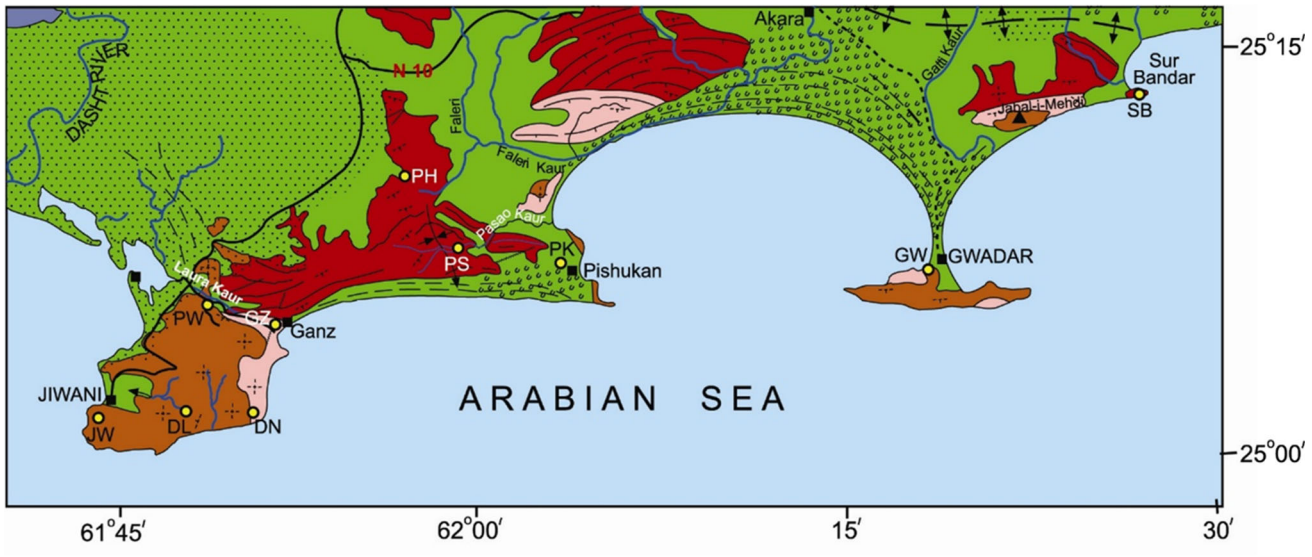

AGE	FORMATION	TH.		DESCRIPTIONS
Holocene	Recent			Alluvial, sand and gravels.
Pleistocene	Jiwani	100ft		Limestone, sandstone and conglomerate.
Plio-Pleistocene	Ormara	3000		Sandy clay with minor conglomerate.
Pliocene	Chatti	4000		Mudstone, sandstone and marl.
Miocene-Pliocene	Talar			Sand/silt-stone, shale and minor limestone.
■ Town	○ Sample site		Road	Stream

Fig. 1 Geological map of study area showing sample sites

Sur Bander areas. Sample locations were determined with the help of Garmin 78 GPS device. All the instruments used in water collection were thoroughly rinsed with the sampled water and stored in 1.5 L pre-sterilized polythene bottles.

3.2 Analytical Techniques

Total dissolved solid contents and pH were measured at the sampling sites using Jenway (Model 370) pH meter. Different physical and chemical parameters of groundwater samples were measured as per standard methods of APHA [19]. Calcium (Ca^{2+}) and magnesium (Mg^{2+}) contents were analyzed by EDTA titration, using Reeder and Patton for Ca and Eriochrome Black T indicators for combined Ca^{2+} and Mg^{2+} while ionic concentrations of Na^{+} and K^{+} were determined using flame-photometer. Carbonate (CO_3^{2-}) and bicarbonate (HCO_3^{-}) concentrations were found by titration against 0.01 N hydrochloric acid (HCl), using phenolphthalein and methyl orange indicators, respectively. Digital chloride meter (Jenway PCLM3) was utilized to measure the chloride content, whereas gravimetric $BaSO_4$ precipitation method was adopted for the assessment of SO_4^{2-} ion.

Fluoride (F^{-}) ions of the groundwater were determined by the specific ion electrode method [20] using a total ionic strength adjusting buffer (TISAB). Nitrate content was measured by selective ion electrode (Orion Model 710A), using NH_4SO_4 Buffer [21].

3.3 Software and Statistical Analysis

The hydrochemical facies evolution diagram (HFE-D) was generated using Microsoft Excel spreadsheet [22]. Stiff and Piper diagrams were generated employing Rock Ware Utilities software. Principal Component Analysis (PCA) and correlation matrix were assessed through SPSS (v. 20).

4 Results and Discussion

4.1 Geochemistry and Seawater Intrusion

Analytical results of physical and chemical parameters of studied samples are given in Table 1 along with Box-Whisker diagrams (Fig. 2) demonstrating minimum, mean, maximum and 25, 50 and 75% quartiles. In general, the abundance of cations display $Na^{+} > Ca^{2+} > Mg^{2+} > K^{+}$ trend (Table 2), however samples from Pishukan (PK) contain more Mg^{2+} than Ca^{2} (Table 1). It is interesting to note that average K^{+}

Table 1 Physical and chemical parameters of the collected samples from study area Gwadar District, Balochistan

Sample. #	Area	Type	Height	pH	TDS	Ca	Mg	Na	K	CO_3	HCO_3	SO_4	Cl	NO_3	F
					mg/l										
JN1	Jiwani	Well	93	6.96	15,150	474	461	4000	300	1	403	1345	6737	118	0.426
DL1	Dedillo	Well	83	7.38	1885	96	57	440	16	12	329	251	638	17	0.600
DL2		Well	99	7.44	1920	92	58	460	18	3	397	240	630	23	0.740
DL3		Well	74	7.55	1810	94	52	440	18	6	360	258	567	21	0.732
DL4		Well	70	7.54	1780	88	54	440	17	6	354	266	531	20	0.749
DL5		Well	100	7.51	1155	84	30	255	15	6	268	156	319	18	0.945
PW1	Panwan	Well	94	7.60	7450	501	294	1585	50	1	171	2015	2517	70	0.709
PW2		Well	300	7.46	3130	172	190	555	50	1	207	1294	638	20	1.030
PW3		Pond	90	7.32	955	92	11	205	9	1	98	209	320	10	0.229
PW4		Pond	100	7.49	2150	188	32	515	18	1	85	493	780	22	0.290
DN1	Daron	Well	302	7.32	1245	100	36	240	18	2	403	93	320	23	0.803
DN2		Well	332	7.23	755	106	6	85	17	1	355	33	140	37	0.318
DN3		Well	349	7.95	1745	128	64	375	20	9	183	265	673	39	1.270
DN4		Well	369	7.55	335	32	23	25	6	2	80	80	70	14	0.586
GZ1	Ganz	Pond	83	7.90	2385	1121	156	6700	200	1	49	2495	10,815	202	0.387
GZ2		Pond	92	9.29	1240	96	18	300	30	3	43	252	469	15	0.222
GZ3		Well	11	7.25	18,430	621	595	4200	4	2	403	1120	8510	950	0.338
PS1	Passu	Pond	83	7.54	2795	312	29	560	15	1	98	1022	710	54	0.170
PH1	Parahetok	Pond		9.38	865	68	7	190	8	1	61	250	248	8	0.194
PK1	Pishukan	Pond	138	7.58	845	128	15	120	7	1	110	280	177	16	0.153
PK2		Pond	130	7.53	1285	122	21	240	20	1	73	460	320	11	0.158
PK3		Well	71	7.25	895	108	15	140	20	1	92	360	140	11	0.152
PK4		Well	70	7.78	7895	128	345	1810	125	6	317	1470	2730	271	1.430
PK5		Well	94	7.96	7655	180	428	1510	325	9	549	1680	2375	1045	2.100
PK6		Well	98	8.17	5215	114	130	1600	110	9	232	647	2340	94	1.630
GW1	Gwadar	Well	224	7.02	3575	216	148	605	150	2	476	1036	886	430	0.362
GW2		Well	66	7.14	8640	232	242	1800	700	1	854	1768	2588	540	0.423
GW3		Well	70	7.11	2250	174	61	400	115	1	317	735	425	121	0.197
GW4		Well	95	7.29	2420	108	114	420	130	2	610	521	496	356	0.325
GW5		Well	290	7.10	4010	216	126	650	300	1	506	1200	992	281	0.299
SB1	Sur Bandar	Well	98	7.06	5275	368	175	1000	200	1	451	1401	1666	685	0.225

content was noted least in all the areas except Gwadar, where it is higher than both Ca^{2+} and Mg^{2+} (Table 1). Potassium is mainly contributed through groundwater by the chemical weathering of K-bearing minerals. In the study area, K^+ concentration ranges from 4.0 to 700.0 with a mean of 97.7 mg/l (Table 2). High K concentrations in Gwadar area are likely derived from the clay fractions exposed there. However, input of K is also suspected from the anthropogenic activities, particularly by the use of NPK-fertilizers. Among the anions Cl^- is the most abundant anion in majority of the locations followed by SO_4^{2-} which may be sourced partly from the gypsum beds associated with Ormara Formation rather than the seawater intrusion [15]. This possibility is supported by the high SO_4^{2-}/Cl^- ratio (meq/l) in the groundwater of the study area which varies from 0.09 to 1.90 with a mean of 0.61 (Table 2) whereas the same ratio is very low (0.1) for seawater. Majority of the samples (24) with intermediate ratio (0.1–1.0) may designate mixing zone and the remaining six samples with high ratio (>1.0) may contain sulfate from the dissolution of gypsum, as indicated by [23]. The HCO_3^- ions occupy the third rank in most of the localities except in Dedillo and Daron areas (Table 1), where Jiwani Formation is exposed.

Average ionic compositions of selected areas are illustrated in Stiff diagram (Fig. 3). Nearly all the samples display dominance of $(Na^+ + K^+)$–Cl^-, while Mg^{2+}–SO_4^{2-} and Ca^{2+}–$(HCO_3^- + CO_3^{2-})$ reveal imbalance in their ionic compositions. Higher Ca^{2+} is noticeable in waters of Ganz

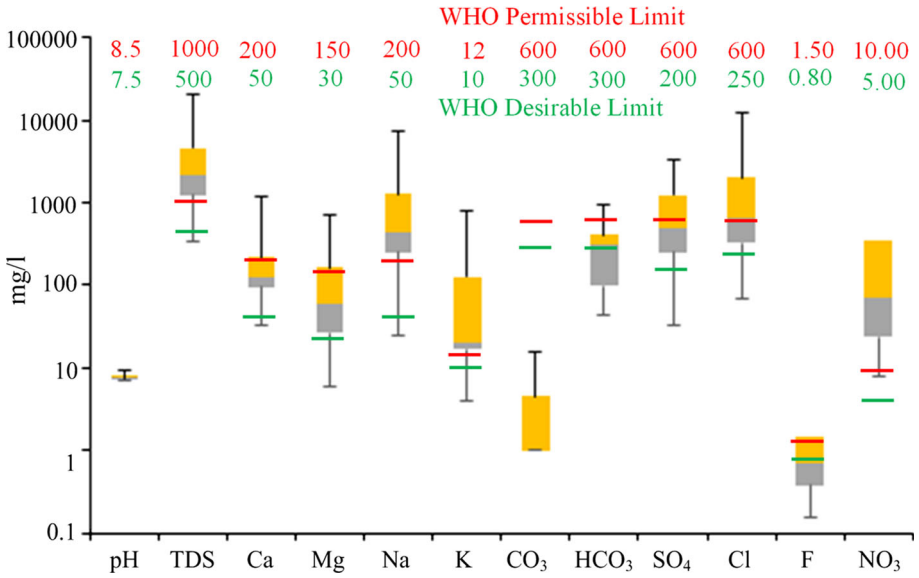

Fig. 2 Box and whisker plot of major ions of groundwater samples of Gwadar area, illustrating important statistics and its comparison with WHO desirable and maximum permissible limits

Table 2 Basic statistical parameters of the groundwater samples of Gwadar, Balochistan

	Av	Min	Max
Depth (m)	137.67	11.00	369.00
pH	7.56	6.96	9.38
TDS (mg/l)	3778.71	335.00	18, 430.00
Ca^{2+} (mg/l)	211.69	32.03	1121.120
Mg^{2+} (mg/l)	128.85	6.08	594.62
Na^{+} (mg/l)	1027.90	25.00	6700.00
K^{+} (mg/l)	97.77	4.00	700.00
CO_3^{2-} (mg/l)	3.06	1.00	12.00
HCO_3^{-} (mg/l)	288.13	42.70	854.00
SO_4^{2-} (mg/l)	764.35	33.00	2495.00
Cl^{-} (mg/l)	1637.64	70.00	10, 815.00
F^{-} (mg/l)	0.58	0.15	2.10
NO_3^{-} (mg/l)	179.00	8.00	1045.00
Ca (meq)	10.56	1.59	55.94
Mg (meq)	10.60	0.50	48.94
Na (meq)	44.71	1.08	291.43
K (meq/l)	2.50	0.10	17.90
CO_3 (meq/l)	0.10	0.03	0.40
HCO_3 (meq/l)	4.72	0.70	14.00
SO_4 (meq/l)	15.92	0.68	51.97
Cl (meq/l)	46.19	1.97	305.07
Na/Cl (meq/l ratio)	1.07	0.55	1.54
Na/K (ionic ratio)	48.84	2.16	1050.00
Mg/Ca (meq/l ratio)	1.04	0.09	4.44
Ca/Mg (ionic ratio)	3.81	0.37	17.45
HCO_3/Cl (ionic ratio)	0.50	0.004	2.53
SO_4/Cl (meq/l ratio)	0.61	0.09	1.90
Mg/Ca (ionic ratio)	0.63	0.05	2.69

Table 2 continued

	Av	Min	Max
Cl/F (ionic ratio)	3920.51	119.45	27, 945.73
$Cl/\sum$ Anions (ionic ratio)	0.47	0.23	0.84
$Na/Na^{+}Cl$	0.40	0.26	0.50
$Ca/Ca^{+}SO$	0.25	0.08	0.76
Chloro Alakline Index 1	−0.154	−0.697	0.372
Chloro Alakline Index 2	−0.067	−0.257	0.212
Revelle Index (RI)	19.67	0.67	364.72

area, whereas high SO_4^{2-} concentration is recorded in Ganz, Gwadar, Panwan and Pishukan samples. Shape of Stiff pattern of Ganz and Panwan areas shows impact of shale, while HCO_3^{-} concentrations are higher than Ca^{2+} in Dedillo and Gwadar areas (Fig. 3). Stiff pattern of Daron area reveals similarity with seawater except SO_4^{2-} which is high due to presence of gypsum beds.

Piper diagram cationic compositions are mainly represented by $Na^{+} + K^{+}$ type, while anions by Cl^{-} and SO_4^{2-}, with few exceptions for $HCO_3^{-} + CO_3^{2-}$ (Fig. 4). Chloride (Cl^{-}) is contributed during seawater intrusion, whereas SO_4^{2-} ions are leached by weathering of gypsum-bearing sedimentary rocks [12] as well as seawater mixing. The diamond shaped area in the Piper diagram [24] signifies four types of hydrofacies and most of the groundwater samples plot into NaCl area. There are also other types of samples, such as Ca^{2+}–Cl^{-} type for DN4 and PK1 samples; Na^{+}–HCO_3^{-} type for DN1 and Ca^{2+}–HCO_3^{-} type for the DN2 locality (Fig. 4).

A number of chemical parameters and indices are used to evaluate origin and processes which modify the nature of water especially seawater intrusions. The molar ratio of

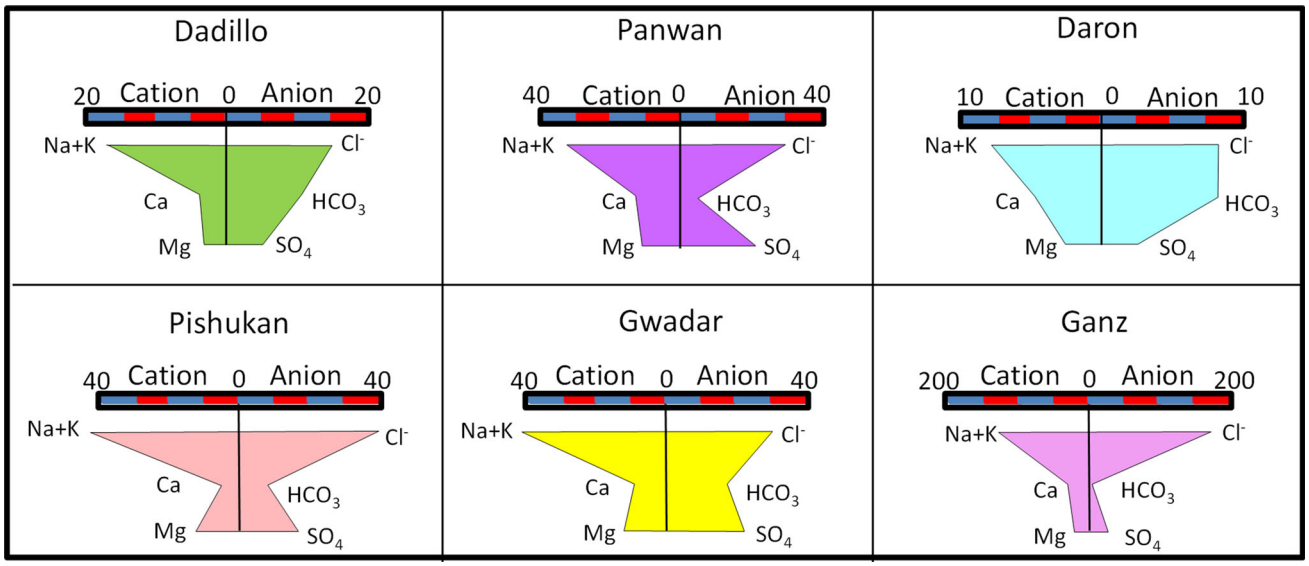

Fig. 3 Stiff diagrams of the groundwater samples, based on average composition of some selected areas

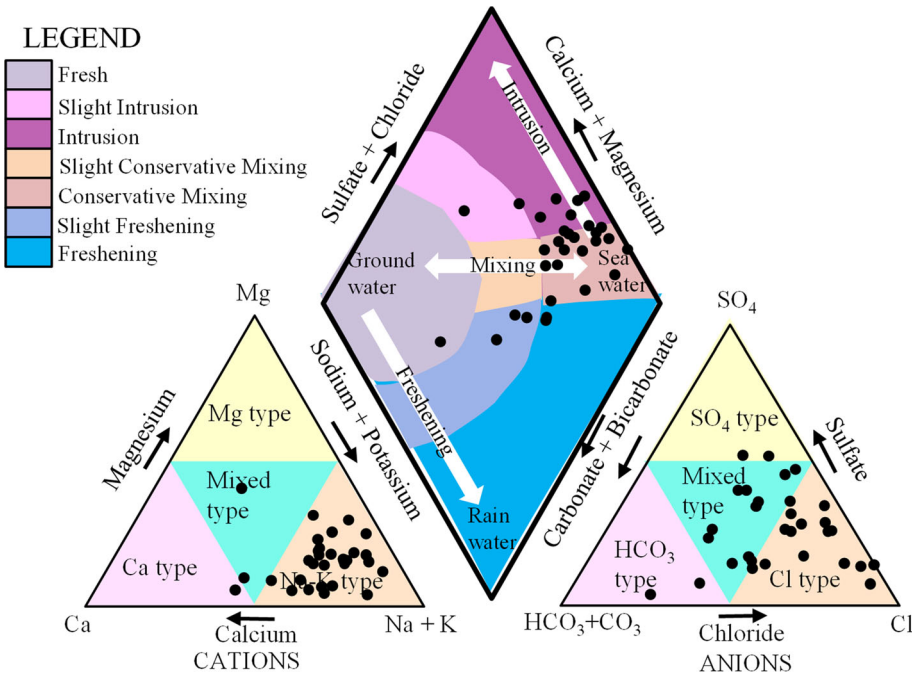

Fig. 4 Groundwater samples of the study area plotted on Piper diagram, showing their types and levels of seawater intrusion

Na^+/Cl^- is important with reference to onshore encroachment of seawater; ratio of <0.86 represents seawater intrusion while the ratio of >1.0 indicates fresh water source [25]. In our study, the molar ratio of Na^+/Cl^- ranges from 0.55 to 1.54 with an average of 1.07 which reveals contamination by seawater to different extents (Table 2). In groundwater, normally the Na^+/K^+ ratio is ≤10 [26], however, in seawater Na^+/K^+ ratio is approximately 27.57. In the study area, Na^+/K^+ ratio of 19% of the samples is >27 exhibiting influence of seawater and 48% of the samples ranging between 27 and 10, indicating mixing zones. Remaining samples have Na^+/K^+ ratio <10 reflecting chemical weathering of clay fractions within Chatti and Ormara formations or due to removal of Na during cation exchange reactions.

Molar ratio of Mg/Ca in groundwater is an important parameter to identify impact of seawater [27]. It may be seen in Fig. 5a that all the samples have Mg^{2+}/Ca^{2+} ratio <2.0, except two samples PK4 and PK5, the sample points of which are quite close to the composition of seawater. Another high Mg^{2+}-bearing group is related to ion exchange mechanism and the Chloro-Alkaline Indices (CAI 1 and 2) of six samples are positive, indicating exchange of Na^+ and K^+

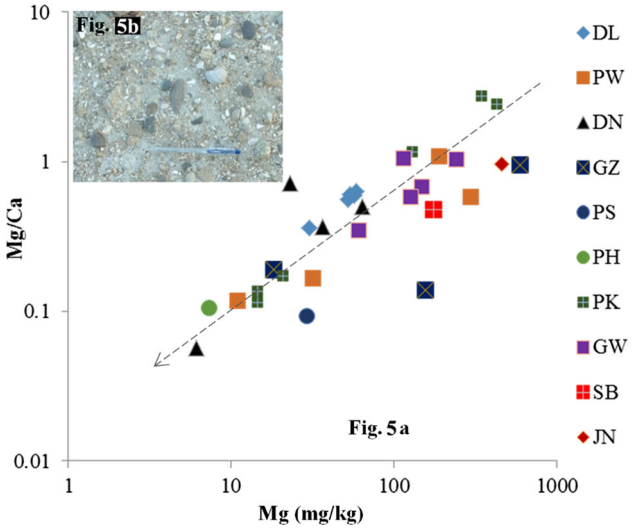

Fig. 5 **a** Mg/Ca versus Mg (mg/kg) relationship, **b** ground exposure NW of Pisukan town, showing pebbles of mafic–ultramafic rocks (*dark colored*)

in groundwater with Mg^{2+} and Ca^{2+} in the aquifer material (Table 2). High Mg^{2+} concentration in the groundwater samples may be due to dissolution of altered mafic and ultramafic rock pebbles of Wakai Group (Fig. 5b). During allochemical serpentinization Mg^{2+} and Ca^{2+} ions are released to the groundwater [28]. Moreover, Mg^{2+}/Ca^{2+} ratio of these samples is proportional to their Mg^{2+} content (Fig. 5a), whereas rest of the samples display a trend of mixing between seawater and groundwater.

Hounslow [29] has referred to certain ionic ratios to signify the process of seawater intrusion as high $Cl^-/\sum$ anions (>0.8) and low $Na^+/Na^+ + Cl^-$ (<0.5) that are related to the effects of seawater impact. The range of $Cl^-/\sum$anions in the samples is between 0.23 and 0.84 and $Na^+/Na^+ + Cl^-$ varies from 0.26 to 0.5, indicating impact of seawater in the area. Hounslow [29] also used $Ca^{2+}/Ca^{2+} + SO_4^{2-}$ ratio to assess seawater intrusion and stipulated that water samples with ratio of <0.3 indicate seawater intrusion. The $Ca^{2+}/Ca^{2+} + SO_4^{2-}$ ratios of studied samples ranged from 0.08 to 0.76, indicating that nearly one-fourth of the samples were fresh water while the rest displayed minor to strong effects of seawater (Table 2). The seawater encroachment and impact of rock weathering may be evaluated on the basis of HCO_3^-/Cl^- ratio [30]. Average HCO_3^-/Cl^- ratio in seawater is ~0.007. It increased in groundwater due to high input of HCO_3^- from the weathering of carbonate rocks and atmospheric interaction. The HCO_3^-/Cl^- ratio of water samples in the study area between 0.004 and 2.53 with a mean of 0.50, reveal a combination of seawater effect and rock weathering (Table 2).

Revelle [31] developed an index to make a distinction between fresh and seawater which is the ionic ratio of $Cl^-/(CO_3^- + HCO_3^-)$ in meq/l. In general-Revelle Index (RI) of freshwater is less than one [32], whereas that of seawater is >200 [33]. Sample (GZ1) has ratio of >200, indicating composition close to seawater. The RI of our samples is 0.67–364.72 with a mean of 19.67 (Table 2), which indicates that coastal groundwater is highly affected by the marine source. According to Revelle [31] grading scheme, only one sample (DN2) was found to be fresh whereas four samples showed low levels of contamination. Thirteen samples had RI values between 2 and 6, four samples between 6 and 10 and eight samples between 10 and 150 indicating moderate to severe impact of seawater contamination.

Kelly [34] and Mikkelson et al. [35] gave new approach to Piper diagram and categorized water into 7 different types. Fresh groundwater and seawater samples occupy the central left and right corners of the diamond part and the area between them represents the conservative mixing zone (mixing without ionic exchange reactions). In case of ion exchange between the groundwater and the aquifer material, the central mixing zone may alter the chemical composition, which deviates due to the mixing of upper and lower areas in the shape of an arc, whereas the upper arc of the diamond indicates intrusion, while downward arc represents freshening; the upper right zone indicates seawater intrusion and its intensity increases toward the top. The plots of major ionic compositions of Gwadar area on Piper diagram signify the impact of seawater intrusion in some of the samples (Fig. 4). Most of the samples (51.6%) were plotted in the conservative mixing zone, while 22.6% of samples represented an initial phase of intrusion and the remainder (25.8%) belonged to the freshwater and mixing zones. The fresh zone samples pertain to inland locations at a height of >300 ft, especially the Daron area. The level of groundwater with respect to mean sea level plays an important role in the influence of seawater intrusion in a coastal area [36]. It is significant that groundwater level is negatively correlated with all the major parameters (Table 3), especially with TDS (−0.345); Na^+ (−0.330) and Cl^- (−0.327).

Giménez-Forcada [37] proposed a hydrochemical facies evolution diagram (HFE-D) to establish the effect of marine environment within the coastal regions. On the basis of major ions chemistry and ion exchange processes prevailing in the area over time, such diagram demarcates two main phases as freshening and intrusion and categorizes waters into 16–32 possible hydrofacies (Fig. 6). The *x*-axis represents base-exchange reactions while *y*-axis signifies mixing phenomenon [22]. Our samples (Fig. 6) were mainly distributed within the freshening phase (80.5%) along with the mixing line indicating an early stage of freshening where mingling of fresh water with seawater occurred (Na^+–Cl^- facies). However, a few samples were found to be relatively more fresh and lay in the Na^+–MixSO_4^{2-}(samples # GW3,

Table 3 Correlation matrix of the hydrochemical parameters

	TDS	Ca^{2+}	Mg^{2+}	Na^{+}	K^{+}	CO_3^{2-}	HCO_3^{-}	SO_4^{2-}	Cl^{-}	F^{-}	NO_3^{-}
pH	−0.121	−0.116	−0.193	−0.053	−0.234	0.215	−0.476	−0.143	−0.063	0.176	−0.188
TDS		0.890	0.780	0.979	0.445	−0.098	0.205	0.782	0.983	0.083	0.547
Ca^{2+}			0.503	0.909	0.257	−0.278	−0.042	0.759	0.902	−0.152	0.336
Mg^{2+}				0.661	0.446	0.059	0.435	0.674	0.694	0.341	0.733
Na^{+}					0.368	−0.082	0.080	0.725	0.992	0.065	0.400
K^{+}						−0.084	0.700	0.628	0.321	0.114	0.534
CO_3^{2-}							0.122	−0.175	−0.090	0.722	0.064
HCO_3^{-}								0.266	0.076	0.200	0.607
SO_4^{2-}									0.685	0.162	0.541
Cl^{-}										0.039	0.436
F^{-}											0.238

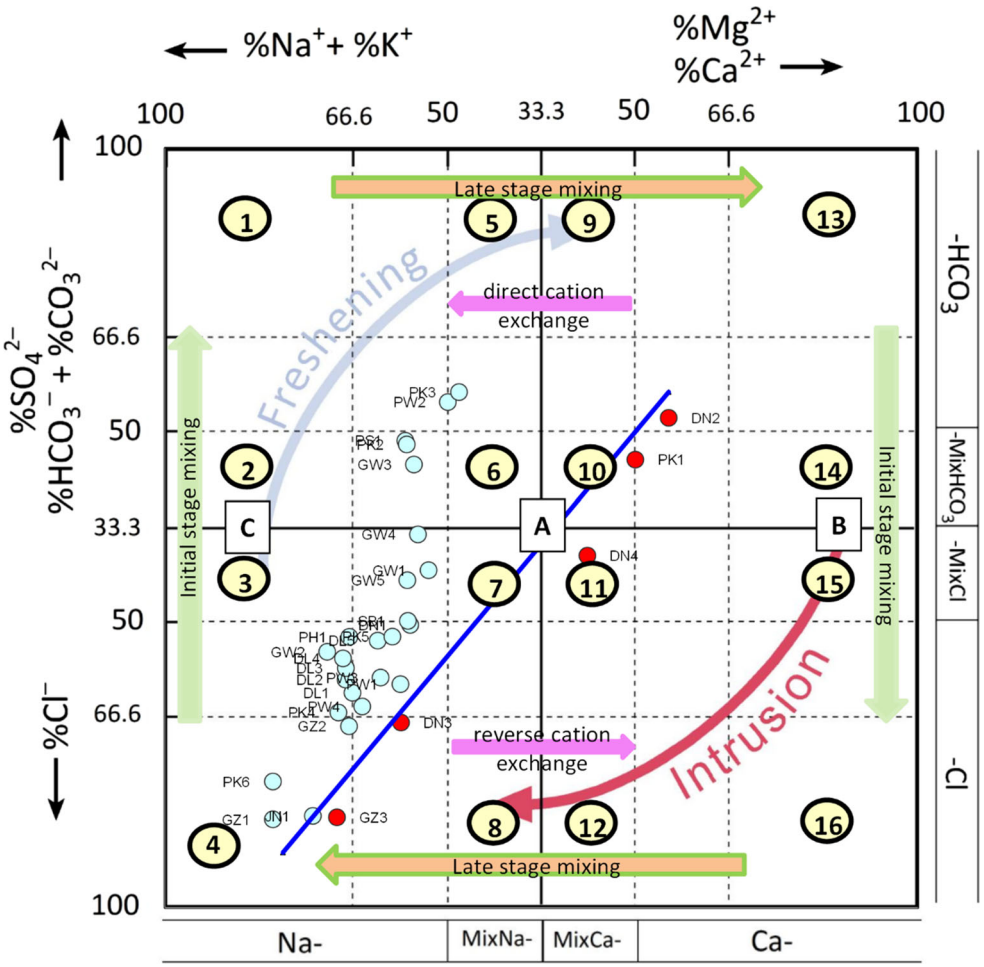

Fig. 6 HFE-diagram showing the main processes occurring in intrusion and freshening stages: **a** mixing between end members: fresh water–sea water; **b** HFE evolution in intrusion period; **c** in freshening period 1: Na–HCO_3/SO_4, 2: Na–$MixHCO_3/MixSO_4$, 3: Na–MixCl, 4: Na–Cl, 5: $MixNa–HCO_3/SO_4$, 6: $MixNa–MixHCO_3/MixSO_4$, 7: MixNa–MixCl, 8: MixNa–Cl, 9: $MixCa–HCO_3/SO_4$, 10: $MixCa–MixHCO_3/MixSO_4$, 11: MixCa–MixCl, 12: MixCa–Cl, 13: $Ca–HCO_3/SO_4$, 14: $Ca–MixHCO_3/MixSO_4$, 15: Ca–MixCl, 16: Ca–Cl

PK2, PS1) and Mix Na^+–SO_4^{2-} (PK3, PW2) facies. The excess SO_4^{2-} in the samples may be due to dissolution of gypsum beds in the study area [12] whereas enrichment of Na^+ in the samples may be due to exchange of Ca^{2+} in the groundwater [38]. Around 19.5% of samples are confined within the intrusion phase (Fig. 6), showing different stages of intrusion with sample # DN2 shows initial stage of mixing as shown by its Ca^{2+}–HCO_3^- facies (i.e., fresh water end member) character on the Piper diagram (Fig. 4). Samples # PK4 and DN4 represent intermediate stage of mixing with slight cation exchange phenomena and are characterized by $MixCa^{2+}$–$MixSO_4^{2-}$ and $MixMg^{2+}$–$MixCl^-$ facies, respectively; with ascendency of Mg^{2+} in sample DN4 is attributed to weathering of serpentinized rocks. Elevation may be a factor for the variation in ion contents of water samples from Daron locality (Table 1). Over all, the studied samples are mostly of Na^+–Cl^- type (either pure or mixed facies) as seen from their positions on the Piper diagram.

The content of F^- ions in the freshwater is generally low (0.1–0.3 mg/l), but it may significantly increase in areas having F-bearing rocks and minerals [39]. The average concentration of F^- ions in the seawater is 1.3 mg/l, and coastal aquifers are often contaminated with F^- [40,41]. In the study area, F^- content ranges from 0.15 to 2.10, with a mean of 0.58 mg/l (Table 2), which may result from the low fluorine content of the sedimentary rocks. Among all, only four samples have F^- values >1.2 mg/l exhibiting influence of seawater intrusion. Chen et al. [42] have used Ca/Mg ratio (av. 0.34) and F^- ions to assess the magnitude of seawater intrusion which is characterized by higher F^- values being associated with low Ca^{2+}/Mg^{2+} ratios. The inverse relation ($r = -0.489$) between Ca^{2+}/Mg^{2+} and F^- in the study area are compatible with the findings of Chen et al. [42].

Smaller size and higher oxidation state of nitrogen (N) enable it to form highly soluble and mobile oxyanions (NO_3^-), whereas geogenic sources of NO_3^- in the groundwater are rather rare, exceptionally in desert areas having deposits like the Chilean Atacama nitrate [43]. Nitrate (NO_3^-) ions are also formed when nitrogenous waste from vegetation, animal manure and sewage water are decomposed by microbial action. Hence, N-bearing fertilizers may be the additional source of NO_3^- contamination in groundwater. Its concentration range is generally low (0–18 mg/l) in the surface water but in the area it has been found between 8 and 1045 mg/l with an average of 179 mg/l (Table 2). The level of NO_3^- in seawater is generally low and hardly exceeds 1 mg/l. Higher NO_3^- in the studied groundwater may be the result of agricultural, refuse dump runoff and contamination from human or animal waste. Average human urine has 39–268 mg/l [44] of NO_3^-, but it may exceed up to 425 mg/l in case of high nitrogenous dyes [45]. Therefore, in the absence of proper sewage facilities in the area, intermingling of sewage waste with the groundwater may be a possibility.

Table 4 Variance of rotated R-mode factor loading matrix in PCA

Variables	Factor I	Factor II	Factor III
Ca (mg/l)	.936	−.011	−.236
Cl (mg/l)	.973	.060	−.004
CO_3 (mg/l)	−.133	−.035	.889
F (mg/l)	.058	.128	.911
HCO_3 (mg/l)	−.015	.933	.136
K (mg/l)	.312	.759	.010
Mg (mg/l)	.690	.479	.271
Na (mg/l)	.974	.062	.003
NO_3 (mg/l)	.432	.669	.230
pH	.031	−.618	.390
SO_4 (mg/l)	.785	.372	−.003
TDS (mg/l)	.969	.211	.016

4.2 Statistical Analysis

Principal Component Analysis (PCA) is applied to detect the effects of anthropogenic and seawater intrusion on the water quality of the study area. The PCA reduces the variables to a smaller number of significant parameters, and hence employed for the analysis of water quality [46–48].

With the help of PCA technique, three factors responsible for the variations of major and minor elements composition in the studied waters has been recognized (Fig. 7; Table 4). The first factor accounts for 42.57% of the variance which clearly identifies the intrusion of seawater in the groundwater due to quite higher positive loadings for Cl^- (0.973), Na^+ (0.974) Ca^{2+} (0.936) and TDS (0.969). The especially high loading of Cl^- is a significant indicator of seawater intrusion in the area [49]. Moreover moderate loadings of SO_4^{2-} (0.785) and Mg^{2+} (0.69) provide genuine support for influx of seawater. Second factor relates to 22.62% of the total variance and the rotated factor matrix shows that highest positive loading has been recorded for HCO_3^- (0.933), K^+ (0.759) and NO_3 (0.67) which appear to be due to surficial reactions. The actual source of high NO_3^- in the groundwater does not correspond to the geology of the area. Kura et al. [50] suggested strong positive loading of NO_3^- as a consequence of anthropogenic pollution. The coastal area contaminated by the use of fertilizers [51,52], may be responsible for the presence of high NO_3^- and K^+ content (Table 3).

The third factor elucidates 16.45% of the total variance showing high positive loadings of CO_3^{2-}(0.889) and F^- (0.911) ions (Fig. 7; Table 4). Such relations have also been observed in other literature [53,54]. High carbonate ion concentrations are indicative of high alkalinity which promotes release of F^- ion from the rocks and soils into the groundwater.

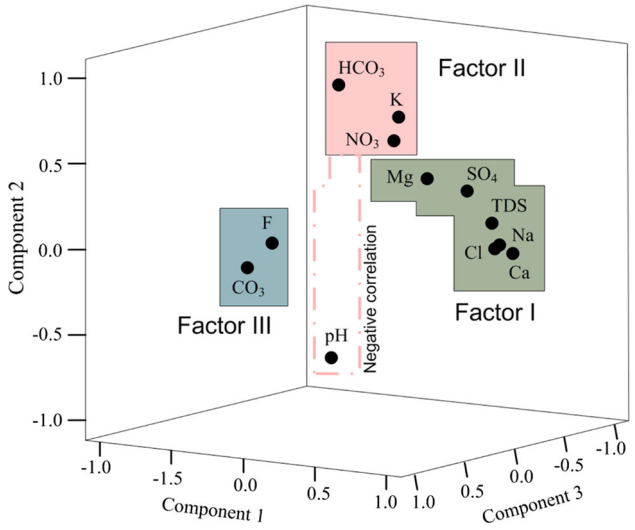

Fig. 7 Rotated loadings showing correlation among pH, TDS and others ions of study area

4.3 Health Risks

Coastal groundwater in the study area contains very high amount of Na^+ ranging from 25 to 6700 mg (with mean of 1028 mg/l; Table 2) which is much higher than maximum permissible limit of WHO [55] (Fig. 2). Concentration of Na is about 500 mg/l which is normal essential daily need for an adult, but higher quantities, especially in warm climate, may cause numerous health hazards. No reliable correlation presently exists between high Na^+ and associated diseases have been confirmed [55]. However, its hazardous impact may initially manifest as headache, nausea, vomiting and twitching in muscles, which persist as hypertension [56] and may silently lead to glaucoma and renal diseases, by interrupting the smooth flow of blood to the brain (ischemic stroke) or rupturing of blood vessels in the brain (hemorrhagic stroke).

Potassium in low quantities (10 mg/l) is beneficial for human health while its excess in drinking water may cause vomiting, nausea, diarrhea, heart disease and coronary artery diseases [57]. The average K^+ content in groundwater of study area is higher (97 mg/l) than WHO maximum permissible limit of 12 mg/l. Potassium concentration of 16% of samples is within the specified limits (Fig. 2). An adult human body requires approximately 530 mg/day Cl^- for proper functioning and impact of its prolonged intake in higher amount is not well documented. Some diseases may arise from the high chloride content, but in fact the actual harm is due to its combination with Na^+ in the form of NaCl [58]. Moreover, the amount of Cl^- ion in the groundwater of study area is much higher, between the range 70–10,815 mg/l with a mean of 1638 mg/l (Table 2).

Some persons are more sensitive to the cathartic effects of high SO_4^{2-} in drinking water [59] and its ingestion in higher quantity may cause dehydration among patients suffering from diarrhea [60]. The cause of these complications being increased serum sulfate levels, due to high production of thyroxine hormone, ultimately appearing as hyperthyroidism [61], whereas higher serum sulfate is also related to kidney failure [62].

The carbonate (CO_3^{2-}) and bicarbonate (HCO_3^-) of Ca^{2+} and Mg^{2+} compounds are mainly responsible for water hardness. In general, adverse health effect of hard water is not documented. However, higher amounts of other elements associated with hard water are mainly responsible for cardiovascular diseases, growth retardation, diabetes and reproductive health. The common assumption regarding water hardness and incidence of urinary stone formation is rather ambiguous. However, a weak association exists between them as formation of oxalates and phosphates of calcium in the kidney (nephrolithiasis) is mainly an environmental problem and may develop due to consumption of hard water [63].

Calcium is essentially required in daily life (1–1.2 g/day) for the development of human skeleton and muscles [64] and its higher quantity may hinder in the absorption of certain toxic elements in the human body. Nearly 29% samples of Gwadar area have high Ca^{2+} contents (>200 mg/l), with no apparent effects on human health. Sample GZ1 has exceptionally high Ca^{2+} (1121 mg/l) which may reduce the absorption of some essential elements in the body. The daily consumption of Mg^{2+} in the body is lesser as compared to Ca^{2+} and its higher amount (>700 mg/l) in the form of sulfate may have a laxative effect. Around 32% water samples are found within WHO desirable limit of Mg^{2+} (30 mg/l), whereas Mg^{2+} contents in 9 samples is higher than the permissible limit (Fig. 2). Good-quality drinking water should have Mg/Ca ratio of ~0.5 [65] while a higher ratio may impose risk of gastric cancer [66]. The Mg/Ca ratios of the samples range between 0.057 and 2.69 (Table 2). Moreover, it may be noted that the average ratio is 0.63 which is close to 0.5 and 14 sampling sites are within the safe limit.

Fluoride (F^-) has a dual biological role in the human body and its deficiency (<0.6 mg/l) in drinking water may cause dental caries. Fluoride content between 0.6 and 1.0 mg/l in drinking water prevents tooth decay and assists in human skeleton development [67], whereas high F^- (>1.5 mg/l) in the groundwater may pose a threat to human health. Long-term exposure to high F^- water is responsible for dental mottling in children, eventually leading to fluorosis of skeleton among adults. In the study area, F^- ranges between 0.152 and 2.1 mg/l (Table 2) and its average concentration is 0.58 mg/l. The current scenario with reference to fluorosis is not yet alarming. However, it still needs an attention to mitigate the endemic problem is necessary. Samples of Pishukan

town (PK4, PK5 and PK6) contain F^- concentrations of 1.43, 1.63 and 2.1 mg/l, respectively, and teeth mottling and joint pain are quite common ailments among its residents. In view of the warm climate of Gwadar area, the F^- permissible limit of 1.0 mg/l seems to be appropriate, since daily consumption of water is high. Bureau of Indian Standards [68] has suggested permissible limit of F^- in drinking water to be 1.0 mg/l, instead of 1.5 mg/l [69] for arid zones.

The concentration of NO_3^- in the study area varies from 8 to 1045 mg/l with a mean of 179 mg/l (Table 2). Nearly 45% of the samples contain NO_3^- ion more than the maximum permissible limit of 45 mg/l (Table 1), which is equivalent to 10 mg/l nitrate-N [70]. Diseases like blue baby syndrome (Methemoglobinemia) and cancers of the digestive tract are often associated with high NO_3^- in the drinking water [71]. However, Powlson et al. [72] have not proved any viable relationship between NO_3^--borne diseases and high NO_3^- intake through drinking water.

5 Conclusions

The groundwater samples from coastal areas of the Gwadar District are mainly saline with high TDS (335–18,430 mg/l, mean 3778 mg/l), the pH varies from 6.96 to 9.38 with an average of 7.56. Sodium (Na^+) is the dominant cation, followed by $Ca^{2+} > Mg^{2+} > K^+$. Regarding anions the pattern of $Cl^- > SO_4^{2-} > HCO_3^- > NO_3^- > CO_3^{2-} > F^-$ is observed. Average ionic composition shows ($Na^+ + K^+$)–Cl^- as the major ionic pair, while Mg^{2+}–SO_4^{2-} and Ca^{2+}–($HCO_3^- + CO_3^{2-}$) are on the lower side. However, the average composition on Stiff diagram has shown an unbalancing for these ions. Some groundwater samples have relatively high content of Mg^{2+}, which may be due the presence of mafic and ultramafic pebbles in the soils of study area. In some locations, NO_3^- is quite high in the groundwater, which may be due to anthropogenic activities.

The Na^+ versus Cl^-, $Na^+/Na^+ + Cl^-$, $Cl^-/\sum$ anions, and Cl/HCO_3^- ratio indicate variable levels of seawater intrusion in the coastal strip of Gwadar area. The composition of groundwater on Piper diagram significantly demonstrates the phenomenon of seawater intrusion. Groundwater samples on hydrochemical facies evolution diagram (HFE-D) are distributed between the phases of freshening and intrusion. The impact of seawater encroachment in the coastal region has been established by principal component analysis. Higher positive loadings of Na^+, Ca^{2+}, Mg^{2+}, Cl^-, SO_4^{2-} and TDS reveal an affiliation with seawater, whereas K, nitrate and bicarbonate form another domain and their relation with pH is found to be negative. The F^- and CO_3^{2-} ions are confined in a separate realm, specifying their source from fresh water.

The average concentrations of Mg^{2+}, CO_3^{2-} and HCO_3^- are found to be within the safe levels of WHO for drinking water, whereas concentrations of remaining ions in the groundwater were very high. Nitrate ions were also found in high proportions, probably due to poor sanitation conditions and the use of fertilizers. Fluoride is high in the samples of Pishukan area. High content of salts and alkalis may cause hypertension and coronary diseases in the inhabitants of the study area. The average SO_4^{2-} content is higher (764 mg/l) than the permissible limit of WHO standard (600 mg/l), which may have led to the common cathartic effects among populace.

References

1. Guo, H.; Jiao, J.J.: Impact of coastal land reclamation on ground water level and the sea water interface. Groundwater **45**(3), 362–367 (2007)
2. Kiro, Y.; Weinstein, Y.; Starinsky, A.; Yechieli, Y.: Groundwater ages and reaction rates during seawater circulation in the Dead Sea aquifer. Geochim. Cosmochim. Acta **122**, 17–35 (2013)
3. Evans, W.C.; Hurwitz, S.; Bergfeld, D.; Lewicki, J.; Huebner, M.A.; Williams, C.F.; Brown, S.T.: Water–rock interaction in the Long Valley Caldera (USA). Procedia Earth Planet Sci. **2013**(7), 252–255 (2013)
4. Frondini, F.; Zucchini, A.; Comodi, P.: Water–rock interactions and trace elements distribution in dolomite aquifers: the Sassolungo and Sella systems (Northern Italy). Geochem. J. **48**, 231–246 (2014)
5. Kim, K.; Rajmohan, N.; Kim, H.; Kim, S.; Wang, G.; Yun, S.; Gu, B.; Cho, M.J.; Lee, S.: Evaluation of geochemical processes affecting groundwater chemistry based on mass balance approach: a case study in Namwon, Korea. Geochem. J. **39**, 357–369 (2005)
6. Qureshi, R.M.; Mashiatullah, A.; Fazil, M.; Ahmad, E.; Khan, H.A.; Sajjad, M.I.: Seawater pollution studies of the Pakistan coast using stable carbon isotope technique. Sci. Vis. **7**, 224–229 (2002)
7. Kassi, A.M.; Khan, A.S.; Kasi, A.K.: Newly proposed Cretaceous–Palaeocene lithostratigraphy of the Ispikan-Wakai area, southwestern Makran, Pakistan. JHES **40**, 25–31 (2007)
8. Grigsby, J.D.; Kassi, A.M.; Khan, A.S.: Petrology and geochemistry of the Oligocene-early Miocene Panjgur Formation and upper Cretaceous Palaeocene Ispikan Formation and Wakai mélange in the Makran Accretionary Belt, southwest Pakistan. In: Abstract, Geological Society of America, Annual Meeting, Colorado, USA, 9th November 2004(GSA Abstracts with Programs), vol. 36(5) (2004)
9. Nicholson, K.; Kassi, A.M.; Grigsby, J.; Khan, A.S.: Petrology and geochemistry of the maficintermediate volcanic Rocks of the Makran Accretionary Wedge, southeast Pakistan. In: Abstract, Geological Society of America, 37th North Central Meeting, Kansas City, Missouri, USA (2003)
10. Kassi, A.M.; Kasi, A.K.; McManus, J.; Khan, A.S.: Lithostratigraphy, petrology and sedimentary facies of the Late Cretaceous–Palaeocene Ispikan Group, southwestern Makran, Pakistan. JHES **46**(2), 49–63 (2013)
11. Naseem, S.; Naseem, S.; Bashir, E.; Shirin, K.; Sheikh, S.A.: Biogeochemical evaluation of *Nannorrhop ritchina*: a Mg-flora from Khuzdar, Balochistan, Pakistan. Chin. J. Geochem. **24**(4), 327–337 (2005)
12. Naseem, S.; Ahmed, P.; Shamim, S.S.; Bashir, E.: Geochemistry of sulphate-bearing water of Akra Kaur Dam, Gwadar, Balochistan,

Pakistan and its assessment for drinking and irrigation purposes. Environ. Earth Sci. **66**(7), 1831–1838 (2012)
13. Malkani, M.S.: Stratigraphy, mineral potential, geological history and Paleobiogeography of Balochistan Province, Pakistan. SURJ (Sci. Ser.) **43**(2), 269–290 (2011)
14. Kazmi, A.H.; Abbasi, I.A.: Stratigraphy and Historical Geology of Pakistan. Graphic Publishers, Karachi (2008)
15. HSC (Hunting Survey Co. Ltd.): Reconnaissance Geology of Part of West Pakistan; a Colombo Plan-Co-Operative Project, Canada (1960)
16. Hussain, J.; Butt, K.A.; Pervaiz, K.: Makran coast: a potential seismic risk belt. Geol. Bull. Univ. Peshawar **35**, 43–56 (2002)
17. MOE: Land Use Atlas of Pakistan, National, Land Use Plan Project, Ministry of Environment, Government of Pakistan (2009)
18. Ghoraba, S.M.; Khan, A.D.: Hydrochemistry and groundwater quality assessment in Balochistan province, Pakistan. IJRRAS **17**(2), 185–199 (2013)
19. APHA: Standard Methods for the Examination of Water and Wastewater, 19th ed. APHA, Washington (1995)
20. Greenberg, E.; Connors, J.; David, J.: Standard Methods for the Examination of Water and Wastewater. APHA, Washington, DC (1998)
21. Clesceri, L.S.; Greenberg, A.E.; Eaton, A.D.: Standard Methods for the Examination of Water and Wastewater, 20th edn. APHA, Washington (1998)
22. Giménez-Forcada, E.; San Román, F.J.S.S.: An excel macro to plot the HFE-diagram to identify sea water intrusion phases. Groundwater (2014). doi:10.1111/gwat.12280
23. Pulido-Leboeuf, P.; Pulido-Bosch, A.; Calvache, M.L.; Vallejos, A.; Andreu, J.M.: Strontium, SO_4^{2-}/Cl^- and Mg^{2+}/Ca^{2+} ratios as tracers for the evolution of seawater into coastal aquifers: the example of Castell de Ferro aquifer (SE Spain). C. R. Geosci. **335**, 1039–1048 (2003)
24. Piper, A.M.: A graphic procedure in the geochemical interpretation of water-analyses. Trans. Am. Geophys. Union **25**, 914–923 (1944)
25. Ekhmaj, A.; Ezlit, Y.; Elaalem, M.: The situation of seawater intrusion in Tripoli, Libya. In: International Conference on Biological, Chemical and Environmental Sciences (BCES-2014) June 14–15, 2014 Penang (Malaysia) (2014)
26. Davis, S.N.; DeWiest, R.J.M.: Hydrogeology. Wiley, New York (1970)
27. Morrel, I.; Pulido-Bosch, A.; Fernandez, R.: Rubio, hydro geochemical analysis of salinization processes in the coastal aquifers of Oropesa, Spain. Environ. Geol. **29**, 118–131 (1986)
28. Bashir, E.; Naseem, S.; Kaleem, M.; Khan, Y.; Hamza, S.: Study of serpentinized ultramafic rocks of Bela Ophiolite, Balochistan, Pakistan. J. Geogr. Geol. Can. **4**(1), 79–89 (2012)
29. Hounslow, A.W.: Water Quality Data: Analysis and Interpretation. CRC Press LLC, Lewis Publishers, Florida (1995)
30. El-Fiky, A.A.: Hydrogeochemical characteristics and evolution of groundwater at the Ras Sudr-Abu Zenima Area, Southwest Sinai, Egypt. JKAU: Earth Sci. **21**(1), 79–109 (2010)
31. Revelle, R.: Criteria for recognition of sea water in ground water. Trans. Am. Geophys. Union **22**, 593–597 (1941)
32. Al-Khatib, M.; Al-Najar, H.: Hydro-geochemical characteristics of groundwater beneath the Gaza Strip. JWARP **3**, 341–348 (2011)
33. Babu, M.M.; Viswanadh, G.K.; Rao, S.V.: Assessment of saltwater intrusion along coastal areas of Nellore District, A.P. IJSER **4**(7), 173–178 (2013)
34. Kelly, D.J.: Development of seawater intrusion protection regulations. In: Proceedings 1st SWIM–SWICA Joint Saltwater Intrusion Conference, pp. 135–146, Cagliari-Chia Laguna, Italy (2006)
35. Mikkelson, N.; Ellis, D.; Beavis, S.; Kirste, D.: The geochemistry of a coastal aquifer system: Merimbula, NSW'. In: Fitzpatrick, R.W., Shand, P. (eds.) CRC LEME Regional RegolithSymposia 2006. CRC LEME, Bentley, Western Australia, pp. 244–248 (2006)
36. Chachadi, A.G.; Ferreira, J.P.L.: Assessing aquifer vulnerability to sea-water intrusion using GALDIT method: part 2—GALDIT indicators description. In: 4th Inter-celtic Colloquium on Hydrology and Management of Water Resources, Guimaräer, Portugal (2005)
37. Giménez-Forcada, E.: Dynamics of seawater interface using hydrochemical facies evolution diagram. Groundwater **48**(2), 212–216 (2010)
38. Gopinath, S.; Srinivasamoorthy, K.: Application of geophysical and hydrogeochemical tracers to investigate salinization sources in Nagapatinam and Karaikal coastal aquifers, South India. Intern. Conf. on water resources, coastal and ocean engineering (icwrcoe 2015). Aquat. Procedia **4**, 65–71 (2015)
39. Casellato, S.; Masiero, L.; Ballarina, L.: Toxicity of fluoride to the freshwater mollusc *Dreissena polymorpha*: effects on survival, histology, and antioxidant enzyme activity. Fluoride **45**(1), 35–46 (2012)
40. El Maghraby, M.M.S.: Geochemical and isotopic evidence of seawater intrusion into the Shallow Pleistocene Coastal Aquifer, West Alexandria, Egypt. Life Sci. J. **11**(7), 749–762 (2014)
41. Arasu, P.T.; Murugan, A.: Physico chemical study on the sea water intrusion in Tuticorin Coastal Area. Int. J. ChemTech. Res. **5**(4), 1824–1828 (2013)
42. Chen, Q.; Song, Z.; Lu, Q.; Wang, M.; Feng, J.; Tian, H.; Liu, J.; Li, X.; Zhang, R.: Fluorine contents and its characteristics of groundwater in fluorosis area in Laizhou Bay, China. Toxicol. Environ. Chem. **94**(8), 1490–1501 (2012)
43. Seo, J.: Solving the Mystery of the Atacama Nitrate Deposits: the use of stable oxygen isotope analysis and geochemistry. JPUR **1**, 38–45 (2011)
44. WHO: Nitrate and Nitrite in Drinking-Water Background Document for Development of WHO Guidelines for Drinking-Water Quality. WHO, Geneva (2011)
45. Radomski, J.L.; Palmiri, C.; Hearn, W.L.: Concentrations of nitrate in normal human urine and the effect of nitrate ingestion. Toxicol. Appl. Pharmacol. **45**(1), 63–68 (1978)
46. Ayeni, A.O.; Soneyen, A.S.O.: Interpretation of surface water quality using principal components analysis and cluster analysis. J. Geogr. Reg. Plan. **6**(4), 132–141 (2013)
47. Wu, Z.Z.; Che, Z.W.; Wang, Y.S.; Dong, J.D.; Wu, M.L.: Identification of Surface Water Quality along the Coast of Sanya, South China Sea. PLoS ONE (2015). doi:10.1371/journal.pone.0123515
48. Bhat, S.A.; Meraj, G.; Yaseen, S.; Pandit, A.K.: Statistical assessment of water quality parameters for pollution source identification in Sukhnag stream: an inflow stream of Lake Wular (Ramsar Site), Kashmir Himalaya. J. Ecosyst. Article ID 898054 (2014)
49. Huang, Y.; Yang, C.; Lee, Y.; Tang, P.; Hsu, W.: Variation of groundwater quality in seawater intrusion area using cluster and multivariate factor analysis. In: Sixth International Conference on Natural Computation (ICNC 2010), pp. 3021–3025. IEEE (2010)
50. Kura, N.U.; Ramli, M.F.; Sulaiman, W.N.A.; Ibrahim, S.; Aris, A.Z.; Mustapha, A.: Evaluation of factors influencing the groundwater chemistry in a small tropical island of Malaysia. Int. J. Environ. Res. Public Health **10**, 1861–1881 (2013)
51. Mtoni, Y.; Mjemah, I.C.; Bakundukize, C.; Camp, M.V.; Martens, K.; Walraevens, K.: Saltwater intrusion and nitrate pollution in the coastal aquifer of Dar es Salaam, Tanzania. Environ. Earth Sci. **70**(3), 1091–1111 (2013)
52. Voudouris, K.; Panagopoulos, A.; Koumantakis, I.: Nitrate pollution in the coastal aquifer system of the Korinthos prefecture (Greece). Glob. Nest: Int. J. **6**(1), 31–38 (2004)
53. Rafique, T.; Naseem, S.; Usmani, T.H.; Bashir, E.; Khan, F.A.; Bhanger, M.I.: Geochemical factors controlling the occurrence of high fluoride groundwater in the Nagar Parkar area, Sindh, Pakistan. J. Hazard Mater. **171**, 424–430 (2009)

54. Khan, S.M.M.N.; Ravikumar, A.: Role of alkalinity for the release of fluoride in the groundwater of Tiruchengode Taluk, Namakkal District, Tamilnadu, India. Chem. Sci. Trans. **2**(S1), S302–S308 (2013)
55. WHO: Sodium in Drinking-Water, Guidelines for Drinking-Water Quality, 2nd ed., vol. 2. Health Criteria and Other Supporting Information. WHO, Geneva (1996)
56. Siegel, L.: Hazard Identification for Human and Ecological Effects of Sodium Chloride Road Salt. State of New Hampshire Department of Environmental Services Water Division Watershed Management Bureau (2007)
57. WHO: Potassium in Drinking-Water Background Document for Development of WHO Guidelines for Drinking-Water Quality. WHO, Geneva (2009)
58. WHO: Chloride in Drinking-Water, Guidelines for Drinking-Water Quality, 2nd ed., vol. 2. Health Criteria and Other Supporting Information. WHO, Geneva (2003)
59. WHO: Sulfate in Drinking-Water Background Document for Development of WHO Guidelines for Drinking-Water Quality. WHO, Geneva (2004)
60. Backer, L.C.: Assessing the acute gastrointestinal effects of ingesting naturally occurring, high levels of sulfate in drinking water. Crit. Rev. Clin. Lab. Sci. **37**, 389–400 (2000)
61. Tallgren, L.G.: Inorganic sulfates in relation to serum thyroxin level and in renal failure. Acta. Med. Scand. **640**, 1S–100S (1980)
62. Cole, D.E.C.; Evrovski, J.: The clinical chemistry of inorganic sulfate. Crit. Rev. Clin. Lab Sci. **37**, 299–344 (2000)
63. Sengupta, P.: Potential health impacts of hard water. Int. J. Prev. Med. **4**(8), 866–875 (2013)
64. Weaver, C.M.; Nieves, J.W.: Calcium and magnesium: role of drinking-water in relation to bone metabolism. In: Calcium and Magnesium in Drinking-Water: Public Health Significance, pp. 94–107 . WHO (2009)
65. Durlach, J.; Bara, M.; Guiet-Bara, A.: Magnesium level in drinking water: its importance in cardiovascular risk. In: Itokawa, Y., Durlach, J. (eds.) Magnesium in Health and Disease, pp. 173–182. J. Libbey & Co Ltd, London (1989)
66. Sakamoto, N.; Shimizu, M.; Wakabayashi, I.; Sakamoto, K.: Relationship between mortality rate of stomach cancer and cerebrovascular disease and concentrations of magnesium and calcium in well water in Hyogo prefecture. Magnes. Res. **10**, 215–223 (1997)
67. Kundu, N.; Panigrahi, M.K.; Tripathy, S.; Munshi, S.; Powell, M.A.; Hart, B.R.: Geochemical appraisal of fluoride contamination of groundwater in the Nayagarh District of Orissa. Indian. Environ. Geol. **41**, 451–460 (2001)
68. BIS: Bureau of Indian Standards Drinking Water-Specifications, 10500. New Delhi, India (2010)
69. WHO: Guidelines for Drinking-Water Quality, 4th ed. WHO, Geneva (2011)
70. WHO: Nitrate and Nitrite Sulfate in Drinking-Water Background Document for Development of WHO Guidelines for Drinking-Water Quality. WHO, Geneva (2011)
71. Manassaram, D.M.; Baker, L.C.; Moll, D.M.: A review of nitrates in drinking water: maternal exposure and adverse reproductive and developmental outcomes. Ciência & Saúde Coletiva **12**(1), 153–163 (2007)
72. Powlson, D.S.; Addiscott, T.M.; Benjamin, N.; Cassman, K.G.; DeKok, T.M.; van Grinsven, H.; L'hirondel, J.L.; Avery, A.A.; van Kessel, C.: When Does Nitrate Become a Risk for Humans? pp. 291–295. American Society of Agronomy, Crop Science Society of America, and Soil Science Society of America (2008)